Origin of trans-ionospheric pulse pairs

H.-C. Wu*
Institute for Fusion Theory and Simulation and Department of Physics, Zhejiang University, Hangzhou 310027, China and
IFSA Collaborative Innovation Center, Shanghai Jiao Tong University, Shanghai 200240, China
(Dated: September 10, 2016)

Trans-ionospheric pulse pairs, associated with lightning, are the most powerful natural radio signals on Earth. Although they were discovered over two decades ago by satellites, their origin remains elusive. Here, we attribute these radio signals to relativistic electrons generated by cloud-to-ground lightning. When these electrons strike the ground, radio bursts are emitted towards space within a narrow cone. This model naturally explains the interval, duration, polarization, coherence, and bimodal feature of the pulse pairs. Based on electron parameters inferred from x-ray observations of lightning, we find that the calculated signal intensity agrees with satellite measurements. Our results can be applied to the development of a global warning system for storms and hurricanes using GPS satellites.

Abrupt increases in the lightning flash rate tend to occur 5-20 minutes prior to severe storms or during hurricane intensification [1]. Thus, it is feasible to use lightning detection as an early warning for storms or hurricanes, thereby reducing injuries, deaths, and property damage. Lightning produces electromagnetic radiation that ranges from radio waves to gamma rays [2]. Investigation into lightning radiation is of fundamental interest and can lead to novel schemes for monitoring lightning and uncovering potential radiation hazards to humans and air vehicles.

Radio bursts in the range of 25 to 200MHz related to lightning have been detected by several satellites, first by ALEXIS [3–5], then by FORTE [6–15], and more recently by Chibis-M [16]. These signals consist of two pulses, typically separated by tens of μs, which travel through the ionosphere to reach the satellites. Hence, they are dubbed trans-ionospheric pulse pairs (TIPPs). These pulse pairs are much stronger than ordinary radio signals from lightning, and they occasionally exceed 1MW in power. They sometimes occur tens of times in a storm, and there have been more than half a million recorded events.

The reflection hypothesis [4] was proposed to explain these pulse pairs. In this scenario, an in-cloud source is assumed to emit a radio burst with a wide pattern. The first pulse in a TIPP is observed along a direct path from the source to the satellite, and the second one corresponds to a signal reflected by the ground. The pulse interval is determined by the source altitude ($\sim$ 10km) and the observation angle. The in-cloud source [17] is then related to the so-called compact intracloud discharge [18, 19].

Although the reflection hypothesis accounts for the typically observed interval of TIPPs, it is confronted with severe challenges. First, this hypothesis implies that, due to reflection loss, the second pulse should be weaker than the first pulse. However, the mean energy ratio of the two pulses remains about unity [3–5], which would require an unlikely surface reflectivity near 100% [4]. In fact, in the sub-100MHz band, the second pulse is occasionally more than twice as strong as the first pulse [4] or even up to one order of magnitude stronger [8]. Moreover, in the $>$ 110 MHz band, the second pulse has more energy than the first pulse for more than half of the events [14]. Second, since the two pulses supposedly originate from the same source, their internal structures should be congruent or somewhat correlated. However, the two pulses in all the $>$ 110 MHz events are found to be completely uncorrelated [14]. Finally, 80% of events seem to occur without compact intracloud discharges [15].

In this paper, we propose an alternative explanation, in which TIPPs are caused by relativistic electrons from cloud-to-ground lightning. When these electrons strike the ground, they induce a radio emission that is beamed towards space and recorded by satellites. This model explains many properties of TIPPs. We remark that there are evidences of an association between these pulse pairs and cloud-to-ground lightning. In a correlation analysis [7], 4083 events were correlated with negative cloud-to-ground strokes, and only 665 events were correlated with intracloud discharges. Moreover, the power of pairs was shown to be proportional to the peak current of cloud-to-ground lightning [10].

Relativistic electron generation is responsible for x-ray emissions observed on the ground [20–23] from stepped leaders of cloud-to-ground lightning. Each leader step emits an x-ray burst during the step formation. This x-ray burst can be a single spike of $\ll 1\mu$s [21], or it consists of several spikes with a total duration of $\sim 1\mu$s [22], corresponding to a single or multiple air breakdowns that form the step.

The consensus [24] on the generation of relativistic electrons is that thermal electrons are initially accelerated to keV by an extremely intense field localized at the leader tip. These electrons then undergo an avalanche and further acceleration in the ambient electric fields between the leader and ground. This mechanism predicts that the electron energy k_e follows the Boltzman-

*huichunwu@zju.edu.cn

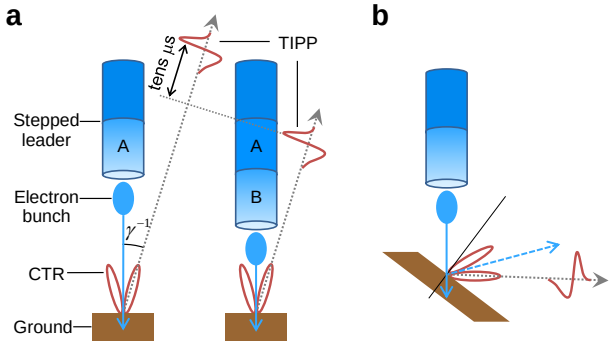

FIG. 1: Model of TIPPs. a, Generation of a TIPP. Two groups of relativistic electrons are produced from the last two steps A and B of a stepped leader. They strike the ground and separately excite the first and second pulses by coherent transition radiation (CTR). b, Scenario for pair detection on the ground. When electrons are obliquely incident on a slope, the radiation can travel along the ground surface.

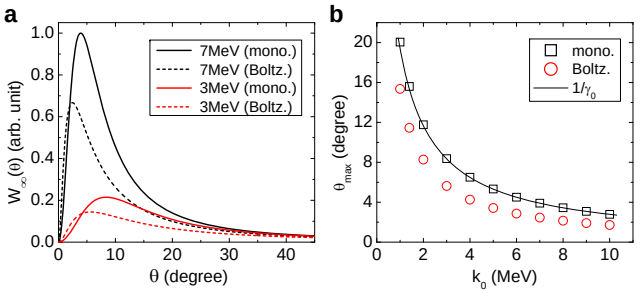

FIG. 2: Radiation distribution. a, Angular distribution of radiation energy for monoenergetic or Boltzmann-distributed electron bunches with electron energies $k_0 = 3$ and 7 MeV. b, The angle of emission peak $\theta_{\max}$ versus k_0.

n distribution $k_0^{-1}\exp(-k_e/k_0)$, where $k_0 = 7.3$MeV is the average energy. A recent analysis [23] shows that $1\times10^{10} - 4\times10^{11}$ collimating electrons can explain the observed x-rays, and they should have a Boltzmann distribution at 7MeV or be monoenergetic from 1 to 10MeV.

Relativistic electrons are expected to have the same profile as x-ray bursts, and they are organized as an isolated electron bunch of $\ll 1\mu$s or a train of electron bunches of totally $\sim 1\mu$s. These electron bunches are directed towards the ground. The range of electrons (1-10MeV) in air is given by $4.4k_{eM}$, where k_{eM} is the energy in MeV. Therefore, electrons at 7MeV can travel 31 meters in the air. The step length of the leaders varies from 3m to 200m [2]. Considering the continuous acceleration by the ambient field, relativistic electrons from the last few steps can reach the ground and excite coherent transition radiation [25]. As depicted in Fig. 1a, two groups of electrons from successive steps A and B account for two pulses in a TIPP. Here, step B refers to the last step nearest the ground.

In regard to the coherent transition radiation, the electron bunch is assumed to have a Gaussian profile $n_{b0}\exp(-r^2/2\sigma_t^2)\exp(-z^2/2\sigma_l^2)$, where n_{b0} is the peak density and σ_t and σ_l are the characteristic radii in the transverse and longitudinal directions, respectively. Simulation [26] shows that the far-field transition radiation is a linearly-polarized bipolar pulse.

Here, we utilize this new model to explain the characteristics of TIPPs. First, the pulse separation of 7.5-110μs [3, 4] found in these pule pairs should equal the step interval, which ranges from 5 to 100μs [2]. Second, two pulses in pairs are either single-spike pulses of 100ns [12], or multi-spike pulses of 2-4μs in total [5]. This bimodal feature corresponds to an isolated electron bunch ($\ll 1\mu$s) or a train of bunches ($\sim 1\mu$s), as directly inferred from x-ray observation. The 100ns pulses are linearly polarized and fully coherent, which is consistent with the coherent transition radiation for a single bunch. The 2-4μs modulated pulses are also polarized [9], but they are strongly modulated and not fully coherent. Electron bunches in the train of $\sim 1\mu$s are randomly distributed, so there is no phase correlation among the discrete radiation emissions from the different bunches. During dispersive propagation in the ionosphere, the stretched radiations overlap and interfere randomly with each other, which degrades their coherence. Third, more electrons from the last step are expected to reach the ground, which explains the trend that the second pulse is more energetic. The second pulse in the 2-4μs modulated case is dominated more by discrete and narrow spikes [14], and this can be due to the reduced travelling diffusion of the train of electron bunches from the last step. Finally, isolated pulse events [4, 16] can occur only when electrons from the last step reach the ground.

Next, we quantitatively discuss the radiation pattern, spectrum, and power of the TIPPs. For a monoenergetic electron bunch normally striking the surface of a perfect conductor with permittivity $\varepsilon = \infty$, the energy distribution of the coherent transition radiation in frequency and angle [27] is given by

$$W_\infty(\omega,\theta) = \frac{r_e mc}{\pi^2}\frac{N^2\beta_0^2\sin^2\theta}{(1-\beta_0^2\cos^2\theta)^2}e^{-\frac{\omega^2}{c^2}(\sigma_t^2\sin^2\theta+\sigma_l^2\beta_0^{-2})}, \quad (1)$$

where ω is the angular frequency, θ is the observation angle with respect to the surface normal, r_e and m are the classic radius and rest mass of electrons respectively, c is the light speed, $N = (2\pi)^{3/2}n_{b0}\sigma_l\sigma_t^2$ is the total electron number, and $\beta_0 = V_0/c$ is the normalized electron velocity. For a general medium, we have $W_\varepsilon(\omega,\theta) \approx \mathcal{R}(\varepsilon)W_\infty(\omega,\theta)$, where $\mathcal{R} = |(\sqrt{\varepsilon}-1)/(\sqrt{\varepsilon}+1)|^2$ is the Fresnel reflectivity (see Methods). In the frequency region of TIPPs, the soil permittivity increases with moisture m_s [28], and it has $\varepsilon_{m_s=15\%} \approx 10-5i$ and $\mathcal{R} \approx 30\%$. Rainfall can dramatically increase the soil moisture and its reflectivity. The Fresnel reflectivity $\mathcal{R} \approx 70\%$ for sea water [29].

Integrating Eq. (1) over ω, we obtain the angular dis-

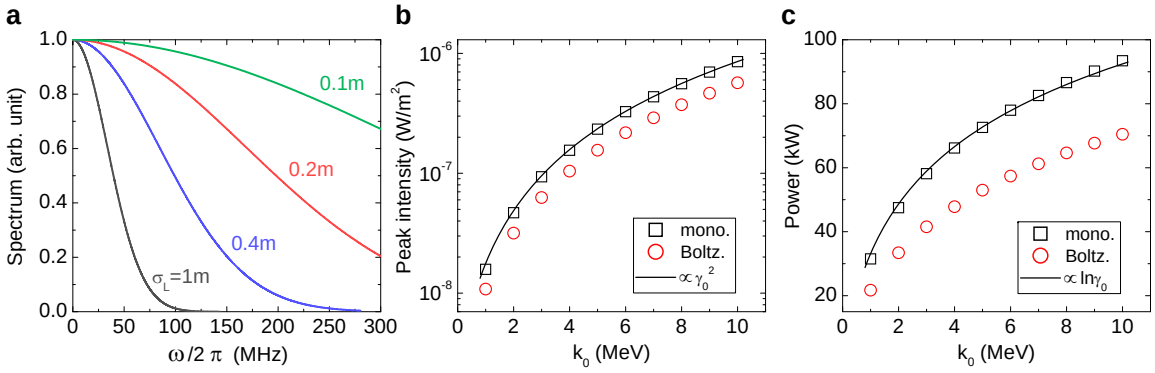

FIG. 3: Spectrum, intensity, and power of radiation. a, Spectrum at the emission peak $\theta_{\max}$ for electron energy $k_0 = 7$ MeV. b, Radiation intensity at $\theta_{\max}$ versus k_0. c. Radiation power versus k_0.

tribution of radiation energy

$$W_\infty(\theta) = \frac{r_e mc^2}{2\pi^{3/2}} \frac{N^2\beta_0^2 \sin^2\theta}{(1-\beta_0^2\cos^2\theta)^2} (\sigma_t^2 \sin^2\theta + \sigma_l^2\beta_0^{-2})^{-\frac{1}{2}}. \quad (2)$$

Figure 2a shows the radiation distribution $W_\infty(\theta)$ for electron bunches with $\sigma_t/\sigma_l = 1$. The radiation is null along $\theta = 0$ and reaches a maximum at an angle of $\theta_{\max} \approx 1/\gamma_0$ (see Fig. 2b), where $\gamma_0 = (1-\beta_0^2)^{-1/2}$ is the relativistic factor. The angle $\theta_{\max} = 3.9^o$ for $k_0 = 7$MeV ($\gamma_0 \simeq 14.7$); thus, the radiation is confined to a very narrow cone and beamed towards space. The ratio σ_t/σ_l affects the emission pattern by the term $\sigma_t^2 \sin^2\theta + \sigma_l^2/\beta_0^2$ in Eq. (2), which is approximately proportional to $(\sigma_t/\sigma_l)^2\gamma_0^{-2} + \beta_0^{-2} \approx 1$ for $\sigma_t/\sigma_l \ll \gamma_0$ near the emission peak ($\theta = \theta_{\max}$). At 7MeV, the radiation pattern changes very little for $\sigma_t/\sigma_l \in [0, 3]$. We also present the results for Boltzmann-distributed bunches with an average energy k_0 (see Methods). These have a smaller $\theta_{\max}$ compared to the monoenergetic case.

Satellites have recorded the spectrum and radiation intensity of TIPPs. Figure 3a displays the spectra from Eq. (1) at the emission peak for monoenergetic bunches with $k_0 = 7$MeV and $\sigma_t/\sigma_l = 1$. The spectral profile remains almost unchanged for $\sigma_t/\sigma_l \in [0, 5]$, and it is also not sensitive to the form of the electron distribution function. The spectral range is proportional to σ_l^{-1}, and it is broader for a shorter bunch. The TIPP spectrum can be flat within the range 28-166MHz [5], which implies $\sigma_l \leq 0.2$m (Fig. 3a). Therefore, the bunch length $L \approx 4\sigma_l \leq 0.8$m, or temporally no longer than 3ns. As discussed above, the single-spike x-ray bursts from the stepped leader are much shorter than 1μs. It has been shown that meter-scale laboratory sparks in air [30] emit x-rays very similar to those in lightning, which are generally sub-10ns [31] and can even be only 1ns [32]. These x-ray observations support that nanosecond electron bunches are generated from the stepped leader.

The radiation intensity can be calculated by $W(\theta)/(TH^2)$, where $T \approx 7.5\sigma_l/c$ is the radiation duration [26] and H is the satellite altitude. Figure 3b displays the radiation intensity at the emission peak versus k_0 for $\sigma_l = 0.2$m, $N = 5 \times 10^{11}$, and $H = 800$km [3, 6]. The monoenergetic 7MeV bunch has a peak intensity of 4.3×10^7W/m^2, which agrees with the measurement from FORTE [8]. The radiation intensity of a Boltzmann-distributed bunch is about 67% that of a monoenergetic bunch. We also can obtain the radiation power by $T^{-1}\int W_\infty(\theta)d\Omega$. In Fig. 3c, the monoenergetic 7MeV bunch has a radiation power of 82kW. Since the radiation power is proportional to N^2, it increases to 1MW for $N = 1.8 \times 10^{12}$. These intensity and power levels are applicable to perfect conductors or metal. For a specific surface (soil or sea), they should be multiplied by the factor $\mathcal{R}$.

Figures 3b and 3c also show that the peak intensity and the power scale with γ_0^2 and $\ln\gamma_0$, respectively, which is the same as the transition radiation of a single electron (see Methods). With increasing electron energy, the radiation cone narrows as γ_0^{-1}, and the peak intensity strengthens rapidly with γ_0^2. As a result, the radiation power/energy increases slowly with γ_0.

The power of a pair of 100ns pulses is typically two orders of magnitude weaker than that of a pair of 2-4μs modulated pulses [12]. According to the transition radiation model, the isolated electron bunch in the 100ns case may contain about ten times fewer electrons than a discrete bunch in a train of electron bunches. This is in accordance with the fact that multi-spike x-ray bursts [22] are stronger than single-spike bursts.

Our model infers that pulse pairs could be detected from the ground. As illustrated in Fig. 1b, when electrons obliquely strike a slope, the radiation cone would be centered around the specular direction, and the maximum radiation can travel along the ground surface. In fact, soon after TIPPs were discovered, pulse pairs with the same characteristics of TIPPs were claimed to be observed on the ground [33]. However, this observation was eventually ascribed to an anthropogenic source [17]. Therefore, ground detection of the pulse pairs remains an open question, and it is considered to be highly possible.

Due to the sporadic nature of lightning, there have only been about 20 ground detections of x-rays from stepped

leaders, and this has limited the ability to interpret electron acceleration in lightning. Coherent transition radiation has been a standard diagnostic tool for measuring the three dimensional structures of electron bunches [34]. Extensive measurements of pulse pairs may shed further light on the mechanism and properties of relativistic electron generation in lightning. To avoid signal dispersion and mode split caused by the ionosphere, pairs can be observed by balloon-carried detectors in the stratosphere.

In conclusion, we reveal that the TIPPs are mainly produced by relativistic electrons from the stepped leader of lightning, and this model can successfully explain many satellite-observed features of the pulse pairs. Notably, the proposed radiation mechanism is distinct from the reflection hypothesis. Distinguishing pulse pairs from compact intracloud discharges will narrow the modelling of the latter. As a signal of lightning activity, our results show that pulse pairs are more easily detected in space. Thus, they can be used for real-time assessment of storms and hurricanes across the globe using GPS satellites [1]. Finally, the TIPP source is on the ground and its potential hazard deserves attention.

Methods

Transition radiation. Transition radiation occurs when electrons penetrate a medium surface. For a single electron normally incident upon the surface of a perfect conductor ($\varepsilon = \infty$), the energy distribution of the transition radiation in frequency and angle [35] is

$$W_{1,\infty}(\omega,\theta) = \frac{r_e mc}{\pi^2}\frac{\beta^2\sin^2\theta}{(1-\beta^2\cos^2\theta)^2}. \tag{3}$$

The maximum radiation is at an angle $\theta_{\max} = \arcsin(1/\beta\gamma) \approx 1/\gamma$ with $W_{1,\infty}(\omega,\theta_{\max}) = \frac{r_e mc}{4\pi^2}\gamma^2$. Since Eq. (3) is independent of ω, the spectrum is flat. The total radiation energy is $W_{1,\infty} \propto \int W_{1,\infty}(\omega,\theta)d\Omega = \frac{r_e mc}{\pi}\left[\frac{(1+\beta^2)}{2\beta}\ln\left(\frac{1+\beta}{1-\beta}\right)-1\right] \approx \frac{2r_e mc}{\pi}\ln\gamma$, where $d\Omega = \sin\theta d\theta d\varphi$ is the differential solid angle and φ is the azimuth angle. Here, all approximations assume $\gamma \gg 1$.

For a bunch of electrons, the transition radiation can be coherent for an electromagnetic component with a wavelength longer than the bunch size. For a Gaussian electron bunch, the energy distribution of the coherent transition radiation in frequency and angle [27] is given by

$$W_\infty(\omega,\theta) = \frac{r_e mc}{\pi^2}N^2 e^{-\frac{\omega^2}{c^2}\sigma_t^2\sin^2\theta}\left[\int \frac{\beta\sin\theta e^{-\frac{\omega^2}{2V^2}\sigma_l^2}}{1-\beta^2\cos^2\theta}f(p)dp\right]^2, \tag{4}$$

where $f(p)$ is the distribution function of the electron momentum p, and it fulfils $\int_0^\infty f(p)dp = 1$. For a monoenergetic bunch with $f(p) = \delta(p-p_0)$, Eq. (4) reduces to Eq. (1). The Boltzmann distribution $k_0^{-1}\exp(-k_e/k_0)$ has $f(p) = \frac{mc^2}{k_0}\frac{p}{\sqrt{1+p^2}}\exp(-\frac{\sqrt{1+p^2}-1}{k_0/mc^2})$, where $k_e = (\gamma-1)mc^2$ is the electron kinetic energy and the momentum $p = P/mc = \gamma\beta$ has been normalized. We numerically calculate Eq. (4) for Boltzmann-distributed bunches.

For a general medium, the expression of radiation distribution for a single electron is very complex [35]. In the limit $\gamma \gg 1$, it is approximately written as $W_{1,\varepsilon}(\omega,\theta) \approx \mathcal{R}(\varepsilon)W_{1,\infty}(\omega,\theta)$, where $\mathcal{R} = |(\sqrt{\varepsilon}-1)/(\sqrt{\varepsilon}+1)|^2$ is the Fresnel reflectivity. Accordingly, $W_\varepsilon(\omega,\theta) \approx \mathcal{R}(\varepsilon)W_\infty(\omega,\theta)$ for the coherent transition radiation. The appearance of $\mathcal{R}$ is because self-fields of a relativistic bunch are predominantly transverse, and coherent transition radiation can be understood as the reflection of the bunch field by the surface [26].

Acknowledgments

This work was supported by the Thousand Youth Talents Plan, NSFC (No. 11374262), and Fundamental Research Funds for the Central Universities. We thank M. Y. Yu for helpful comments.

[1] Hamlin, T. *et al.* Space- and ground-based studies of lightning signatures. Betz, H. D. *et al.* (eds.), *Lightning: Principles, Instruments and Applications* (Springer, Germany, 2009).
[2] Rakov, V. A. & Uman, M. A. *Lightning: Physics and Effects* (Cambridge Univeristy Press, Cambridge, 2003).
[3] Holden, D. N., Munson, C. P. & Devenport, J. C. Satellite observations of transionospheric pulse pairs. Geophys. Res. Lett. **22**, 889-892 (1995).
[4] Massey, R. S. & Holden, D. N. Phenomenology of transionospheric pulse pairs. Radio Sci. **30**, 1645-1659 (1995).
[5] Massey, R. S., Holden, D. N. & Shao, X.-M. Phenomenology of transionospheric pulse pairs: Further observations. Radio Sci., **33**, 1755-1761 (1998).
[6] Jacobson, A. R. *et al.* FORTE observations of lightning radio-frequency signatures: Capabilities and basic results. Radio Sci. **34**, 337-354 (1999).
[7] Jacobson, A. R. *et al.* FORTE radio-frequency observations of lightning strokes detected by the national lightning detection network. J. Geophys. Res. **105**, 15653 (2000).
[8] Tierney, H. E. *et al.* Transionospheric pulse pairs originating in maritime, continental, and coastal thunderstorms: Pulse energy ratios. Radio Sci., **37**, 11-1–11-7 (2002).
[9] Shao, X.-M. & Jacobson, A. R. Polarization observations of lightning-produced VHF emissions by the FORTE satellite. J. Geophys. Res. **107**, 4430 (2002).
[10] Light, T. E. L. & Jacobson, A. R. Characteristics of impulsive VHF lightning signals observed by the FORTE satellite. J. Geophys. Res. **107**, 4756 (2002).
[11] Jacobson, A. R. Relationship of intracloud lightning ra-

diofrequency power to lightning storm height, as observed by the FORTE satellite. J. Geophys. Res. **108**, 4202 (2003).

[12] Jacobson, A. R. & Light, T. E. L. Bimodal radio frequency pulse distribution of intracloud-lightning signals recorded by the FORTE satellite. J. Geophys. Res. **108**, 4266 (2003).

[13] Jacobson, A. R. How do the strongest radio pulses from thunderstorms relate to lightning flashes. J. Geophys. Res. **108**, 4778 (2003).

[14] Jacobson, A. R., Holzworth, R. H. & Shao, X.-M. Observations of multi-microsecond VHF pulsetrains in energetic intracloud lightning discharges. Ann. Geophys. **29**, 1587-1604 (2011).

[15] Jacobson, A. R. & Light, T. E. L. Revisiting narrow bipolar event intracloud lightning using the FORTE satellite. Ann. Geophys. **30**, 389-404, (2012).

[16] Dolgonosov, M.S. *et al.* Solitary trans-ionospheric pulse pairs onboard of the microsatellite Chibis-M. Adv. Space Res. **56**, 1177-1184 (2015).

[17] Smith, D. A. *et al.* A distinct class of isolated intracloud lightning discharges and their associated radio emissions. J. Geophys. Res. **104**, 4189-4212 (1999).

[18] Le Vine, D. M. Sources of the strongest RF radiation from lightning. J. Geophys. Res. **85**, 4091-4095 (1980).

[19] Nag, A. & Rakov V. A. Compact intracloud lightning discharges: 1. Mechanism of electromagnetic radiation and modeling. J. Geophys. Res., **115**, D20102 (2010).

[20] Moore, C. B. *et al.* Energetic radiation associated with lightning stepped-leaders. Geophys. Res. Lett. **28**, 2141-2144 (2001).

[21] Dwyer, J. R. *et al.* X-ray bursts associated with leader steps in cloud-to-ground lightning. Geophys. Res. Lett. **32**, L01803 (2005).

[22] Howard, J. *et al.* RF and X-ray source locations during the lightning attachment process. J. Geophys. Res. **115**, D06204 (2010).

[23] Babich, L. P. *et al.* Analysis of the experiment on registration of X-rays from the stepped leader of a cloud-to-ground lightning discharge. *J. Geophys. Res.* **118**, 2573 (2013).

[24] Dwyer, J. R., Smith, D. M. & Cummer, S. A. High-energy atmospheric physics: terrestrial gamma-ray flashes and related phenomena. Space Sci. Rev. **173**, 133-196 (2012).

[25] Happek, U., Sievers, A. J. & Blum, E. B. Observation of coherent transition radiation. Phys. Rev. Lett. **67**, 2962-2965 (1991).

[26] Wu, H.-C. Relativistic-microwave theory of ball lightning. Sci. Rep. **6**, 28263 (2016).

[27] Zheng, J. *et al.* Spectrum of transition radiation from hot electrons generated in ultra-intense laser plasma interaction. Phys. Plasma **9**, 3610-3616 (2002).

[28] Saarenketo, T. *et al.* Electrical properties of water in clay and silty soils. *J. Appl. Geophys.* **40**, 73 (1998).

[29] Kachan, M. V. & Pimenov, S. F. Remote sensing of water at decameter wavelengths. *IEEE Trans. Geosci. Remote Sensing* **35**, 302-307 (1997).

[30] Dwyer, J. R. *et al.* X-ray bursts produced by laboratory sparks in air. *Geophys. Res. Lett.* **32**, L20809 (2005).

[31] Nguyen, C. V., J van Deursen, A. P. & Ebert, U. Multiple x-ray bursts from long discharges in air. *J. Phys. D* **41**, 234012 (2008).

[32] Kochkin, P. O., J van Deursen, A. P. & Ebert, U. Experimental study on hard x-rays emitted from meter-scale negative discharges in air. J. Phys. D **48**, 025205 (2015).

[33] Smith, D. A. & Holden, D. N. Ground-based observations of subionospheric pulse pairs. Radio Sci. **31**, 553-571 (1996).

[34] Shibata, Y. *et al.*, Diagnostics of an electron beam of a linear accelerator using coherent transition radiation. Phys. Rev. E **50**, 1479-1484 (1994).

[35] Landau, L. D. & Lifshitz, E. M. *Electrodynamics of Continuous Media* (Pergamon, Oxford, 1984).